THE JOURNAL OF PHYSICAL CHEMISTRY B

Article

pubs.acs.org/JPCB

Protonated Water Dimer on Benzene: Standing Eigen or Crouching Zundel?

Huan Wang and Noam Agmon*

The Fritz Haber Research Center, Institute of Chemistry, The Hebrew University of Jerusalem, Jerusalem 91904, Israel

Supporting Information

ABSTRACT: Protonated water clusters that are hydrogen-bonded to a neutral benzene molecule are a reductionist model for protons at hydrophobic surfaces, which are of fundamental importance in biological energy transduction processes. Of particular interest is the protonated water dimer ("Zundel ion") on benzene, whose gas-phase messenger IR spectrum has been previously interpreted in terms of an asymmetric binding of the protonated water dimer to the benzene ring through a single water molecule. This "standing Eigen" isomer has a hydronium core. We have found an alternative "crouching Zundel" isomer, which attaches to the benzene ring symmetrically via both of its water molecules. When Ar-tagged, it has an IR spectrum in much better agreement with experiment than the standing Eigen isomer, particularly at the lower frequencies. These conclusions are based on static harmonic (and anharmonic) normal-mode analysis using density functional theory with various (dispersion corrected) functionals and particularly on dynamic anharmonic spectra obtained from the dipole autocorrelation functions from classical ab initio molecular dynamics with the BLYP, PBE, and B3LYP functionals. Possible implications to protons on water/organic-phase interfaces are discussed.

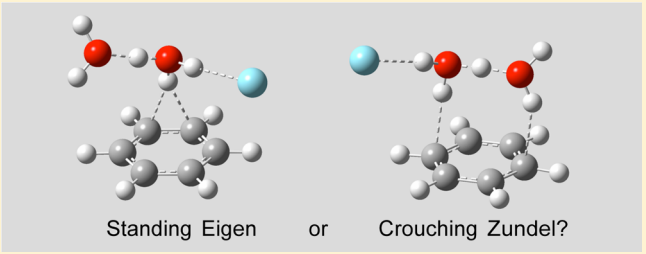

INTRODUCTION

Protons in aqueous solutions participate in a myriad of acid–base and enzymatic reactions, in processes such as corrosion, acid-rain formation, and charge conduction in putative hydrogen cells. In living cells (or organelles within), the interface between hydrophobic membranes and the aqueous phase is pivotal in energy transduction processes. Energy (from metabolism or light absorption) drives membranal proton pumps, and the pH gradient is then utilized to synthesize ATP.[1] Recent experiments suggest that the pumped protons may be conducted in the water layer along the water–oil interface for long distances, but the forces that hold them there remain an enigma.[2,3] A simple Gaussian-exponential function describes the time-dependence of the membranal proton migration-release processes.[4] Experiments[5] and simulations[6,7] show that water surface is acidic, that hydronium ions migrate also toward water–organic solvent interfaces[8] where there is a slight preference for the positive charge to delocalize between two water molecules (the "Zundel cation", $H_5O_2^+$).[9] However, simulations do not yet reproduce the long proton retention times on the surface that are coupled to its fast diffusion therein.[10]

Conceptually, at least, protonated water clusters in the gas-phase may correspond to elementary molecular components of aqueous acidic solutions.[11] Their study has gained momentum following the development of the "messenger" method, where gas-phase cluster ions are "tagged" by noble gas atoms (e.g., Ar) that photodissociate upon absorption of an infrared (IR) photon, so that the mass-spectrometric abundance of the daughter ion reports on the IR absorption probability.[12] However, the correspondence between cluster and liquid structures turns out not to be as simple as anticipated. For example, in liquid water the triply hydrated hydronium, $H_3O^+(H_2O)_3$ (the "Eigen cation"), is thought to be the dominant protonated water structure, which is stabilized by static and dynamic distortions (the "special pair dance").[13] It was natural to expect that the protonated water tetramer, $H^+(H_2O)_4$, forming in the molecular beams, is a prototype Eigen cation. This is indeed how all its predissociation IR spectra have been interpreted.[12,14−19] Yet there remained unassigned IR peaks below 2000 cm^{-1}, which are typical to a shared proton in the Zundel cation.[14,15,20] Ab initio molecular dynamic (AIMD) simulations recently showed that these peaks could be accounted for with a linear 4-water chain isomer, which has a Zundel rather than an Eigen core.[21] For the protonated water pentamer, a linear isomer was again required to explain the bands below 2000 cm^{-1}, and it has a central H_3O^+ moiety with bond lengths intermediate between those of an Eigen and Zundel cations (the "E-Z cation").[22] Thus, for small clusters in the gas phase, perhaps due to limited solvation, a shared-proton state might be more prevalent than in bulk water.

Special Issue: Photoinduced Proton Transfer in Chemistry and Biology Symposium

Received: September 5, 2014
Revised: December 16, 2014
Published: December 17, 2014

DOI: 10.1021/jp509004j
J. Phys. Chem. B 2015, 119, 2658−2667

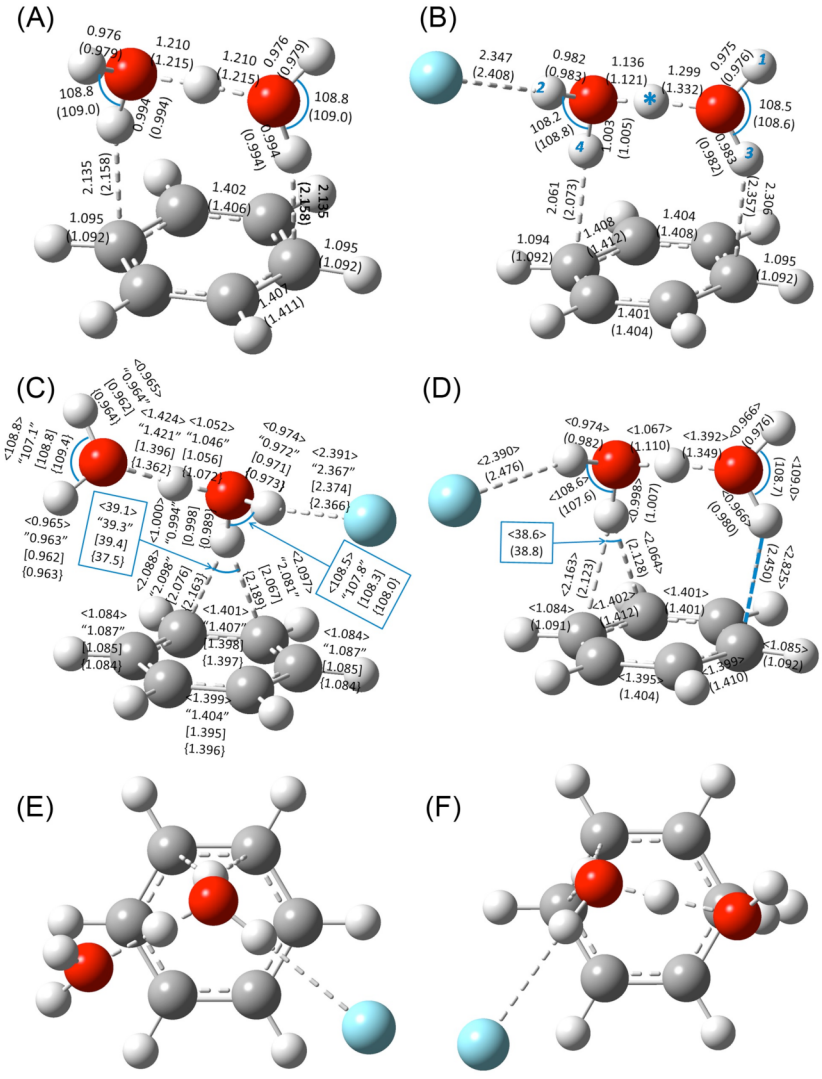

Figure 1. Optimized geometry of the $H_5O_2^+$–benzene cluster, with and without Ar, optimized in Gaussian 09 using DFT with five different (dispersion corrected) functionals, and MP2(fc), combined with the same 6-311+G(d,p) basis set. The clusters are (A) $H_5O_2^+$(bz) and (B–F) $H_5O_2^+$(bz)Ar. The isomers found by geometry optimization are (A and B) cZ from PBE or BLYP; (C) sE from PBE0, B3LYP, M06-2x or MP2(fc); (D) E-Z from BLYP or B3LYP; and (E and F) top views of (C) and (D), respectively. Diatomic distances (in angstroms) and triatomic angles (in degrees) are given in the following notation: PBE, [PBE0], (BLYP), <B3LYP>, {M06–2x}, and "MP2(fc)". H-bond distances are given next to the dashed gray lines (blue line when the cutoff is exceeded). Oxygens colored red and Ar cyan. Panel (B) also labels (in blue) the five hydrogen atoms of the Zundel moiety.

With the vision of eventually explaining proton solvation at aqueous hydrophobic interfaces, Duncan and collaborators have conducted a seminal study of the IR spectra of protonated-water benzene (bz) clusters, $H^+(H_2O)_n(bz)_m$, n and m = 1, ..., 4.[23] We focus herein on the $H^+(H_2O)_2$(bz) cluster, to which a single Ar atom was attached in the mass-spectrometric experiments. It was noted that this cluster has spectral features akin to the Zundel cation and was therefore suggested that it constitutes a "zundel ion attached to neutral benzene via a π-hydrogen bond".[23] On the basis of optimized quantum chemistry structures with either density functional theory (DFT) with the B3LYP functional or the second order Møller–Plesset (MP2) perturbation method, this water–bz attachment was conceived to occur via a single water hydrogen, similar to Figure 1C. However, it was noted that the proton between the two water oxygen atoms (to be denoted by H*) is not equally shared between them as in the Zundel cation but is rather close (1.046 Å, MP2) to the water attached to the bz ring. Thus, this complex is more accurately described as a hydronium (H_3O^+) solvated by bz, H_2O, and Ar, namely an Eigen cation with three different first-shell ligands. We call it a "standing Eigen" (sE) isomer because the protonated water dimer stands on the bz ring through only one of its water molecules.

The experimental IR predissociation spectrum (Figure 3 of ref 23) showed two pronounced bands below 2000 cm^{-1} that might be typical to the Zundel cation, though somewhat blue-shifted (1488 and 1820 cm^{-1}). This experimental spectrum is reproduced in Figure 2A below. The IR spectrum of the sE isomer was calculated with the DFT/B3LYP and MP2 quantum chemistry methods in the harmonic approximation. This did not yield any sizable peaks below 2000 cm^{-1} (compare with Figure 2D), in contrast to the experiment. In addition, the calculation produced a strong shared-proton (H*) peak at 2260 cm^{-1}, which is "far from any measured band".[23] It was assumed there, but not demonstrated, that the inclusion of anharmo-

DOI: 10.1021/jp509004j
J. Phys. Chem. B 2015, 119, 2658–2667

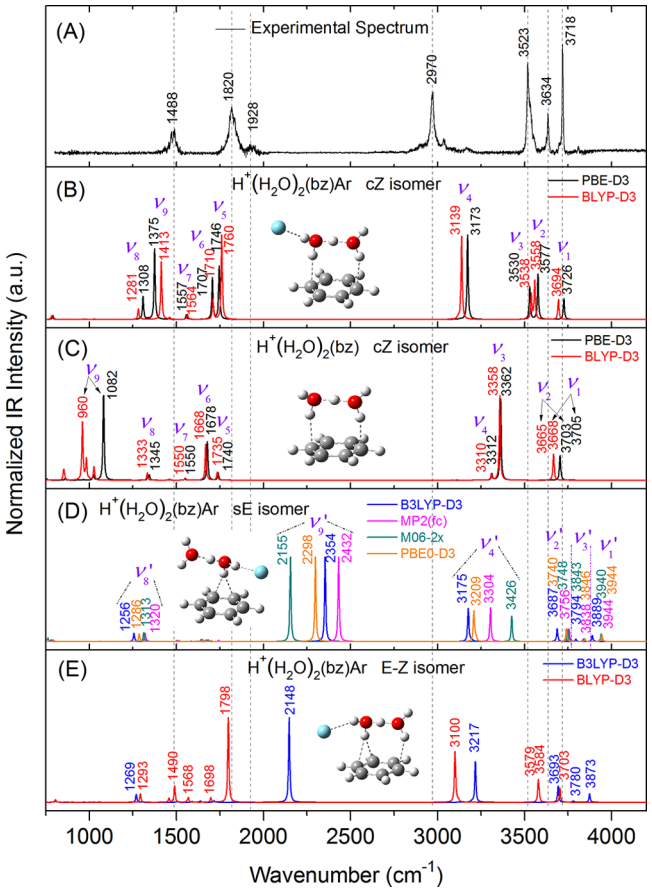

Figure 2. Infrared spectrum of the protonated water dimer−benzene cluster. (A) Experimental Ar-tagged spectrum at 50 K. Data from ref 23 (Figure 3). (B−E) Harmonic normal-mode IR spectra calculated in Gaussian 09 with the indicated quantum chemistry methods (for the optimized geometries obtained with the same respective methods and shown in Figure 1). (B and C) The crouching Zundel isomer (B) with and (C) without an attached Ar atom, from the PBE-D3 (black line) and BLYP-D3 (red line) functionals. (D) The standing Eigen isomer from B3LYP-D3 (blue line), MP2(fc) (magenta line), PBE0-D3 (orange line), and M06−2x (cyan line). (E) The E-Z isomer from BLYP-D3 (red line) and B3LYP-D3 (blue line). Peak frequencies, in cm^{-1}, are noted for the 9 bands listed in Table 2 and Tables S34 and S35 of the Supporting Information.

nicities will down-shift the experimental shared-proton band to 1488 cm^{-1}. We will argue below that such a shift is excessive for an OH bond whose length is under 1.05 Å.

In order for the $H_5O_2^+$ moiety to behave as a (nearly) symmetric Zundel cation, it should be placed symmetrically on the bz ring, with one hydrogen-bond (H-bond) for each of its two water molecules. Indeed, we have found such an isomer when either the PBE or BLYP (rather than the B3LYP) functionals are utilized in the DFT optimization, see Figure 1, panels A and B. The central shared proton (H*) is now placed (nearly) symmetrically between the two oxygen atoms, leading to the "crouching Zundel" (cZ) isomer.

If the distinction between these two isomers can be projected into the liquid phase then the first might foster an Eigen ion at the interface, whereas the second suggests the predominance of the Zundel cation there. Due to this possibly significant distinction, we were motivated to investigate the IR spectra of both isomers theoretically, by computing both their static, normal-mode spectra (without and with anharmonic corrections) and their dynamic (and hence inherently anharmonic) spectra.

For floppy systems such as H-bonded clusters, normal-mode spectra may be problematic because the system does not possess a single deep minimum around which it oscillates but rather meanders over a relatively flat landscape. This is better sampled by molecular dynamics (MD) trajectories, from which a dipole-moment autocorrelation function can be calculated and Fourier transformed to yield the IR spectrum.[24] While empirical force fields are not spectroscopically accurate, AIMD simulations in which one solves the electronic Schrödinger equation every time step (usually at the DFT level) do produce sufficiently accurate forces for solving the Newton equations for the nuclei.[25] This has been applied, for example, to protonated peptides[26−28] and medium-sized protonated water clusters[11,21,22,29−31] with encouraging results.

Here we show that, in contrast to the static ab initio spectra, DACF from AIMD simulations (at 50 K) consistently point to cZ as the dominant isomer, and its IR spectrum is in semiquantitative agreement with experiment.

METHODS

The geometry of the $H^+(H_2O)_2(bz)$ cluster, with and without an attached argon atom, was first optimized with the Gaussian 09 program package,[32] starting from two initial guesses for the cluster geometry: a "standing Eigen" (sE) isomer, with only one of the $H_5O_2^+$ H atoms H-bonding to the bz ring, and the "crouching Zundel" (cZ) isomer, with one H atom from each of the two water molecules attached to two *para* carbon atoms of the bz ring.

In DFT, we have used five (dispersion corrected) functionals: PBE-D3,[33] PBE0-D3,[34] BLYP-D3,[35] B3LYP-D3,[36,37] and M06-2x.[38] In addition, a MP2 calculation with frozen core [MP2(fc)] was performed. The Pople 6-31G(d) basis set was used for preoptimization.

Three isomers were thus generated (see Results). To confirm their stability, all three were reoptimized with the 6-311+G(d,p) basis set. No further isomers were thus obtained. Tight convergence criterion was used for the SCF procedure and ultrafine grid for two-electron integrals and their derivatives. The optimized structures are shown in Figure 1, with coordinates detailed in Tables S1−S16 of the Supporting Information.

The (static) harmonic and anharmonic spectra were then calculated at each of the above optimized geometries with the corresponding quantum method (Tables S17−S32 of the Supporting Information). As reported elsewhere,[39] augmentation of the basis set from 6-31+G(d) to 6-311+G(3df,3pd) is not crucial for the evaluation of the anharmonic IR spectra of the protonated water trimer and tetramer. Consequently, the 6-311+G(d,p) basis should be sufficiently accurate to describe our system.

Anharmonic frequency analysis was based on the second-order vibrational perturbation theory (VPT2).[40] While the determination of harmonic normal-mode frequencies requires the force constant matrix (second partial derivatives of the potential), VPT2 requires partial derivatives up to the fourth order. For floppy systems, it does not always converge.

Classical AIMD simulations were performed in the CP2K/Quickstep software package,[41] see http://www.cp2k.org/quickstep. This code describes the electronic structure using DFT with a mixed Gaussian and plain wave basis. Three functionals were tested, PBE, BLYP, and B3LYP, all with

DOI: 10.1021/jp509004j
J. Phys. Chem. B 2015, 119, 2658−2667

Grimme's third generation dispersion correction (DFT-D3).[42] The augmented triple-ζ valence polarization (aug-TZVP) basis set with the corresponding Goedecker-Teter-Hutter (GTH) pseudopotentials[43] were used for all atoms except Ar, for which the DZVP-GTH basis set was used. The plane wave energy cutoff was set to 300 Ry. Self-interaction correction (SIC) was applied with the Martyna-Tuckerman Poisson equation solver.[44] The orbital transformation (OT) method was applied for faster convergence,[45] with the convergence criterion of 1×10^{-5} a.u. at every MD step.

In the PBE and BLYP simulations, the time step was set to 0.2 fs to account for the fast hydrogen atom motions, which had masses of 1 amu. For B3LYP simulations (which require considerably longer computer times), the time step was 0.5 fs and all hydrogen masses were set to 2. The OH frequencies were then scaled by the square-root of the OD/OH reduced mass ratio,[11,21] $(2 \times 17/18)^{1/2} = 1.37$. At each time step, the interatomic forces were computed from the electron density using the Hellmann−Feynman theorem, and the atoms then propagated classically, by solving Newton's equations in this force field.

The initial coordinates for the simulations were taken from the Gaussian 09 optimizations described above. The accuracy of the initial structures is not crucial here because they were subsequently equilibrated in CP2K for at least 6 ps in the canonical (NVT) ensemble. The target temperature was 50 K (the temperature estimated for the molecular beam), maintained by the Nosé−Hoover chains thermostat.[46] After equilibration, each trajectory was continued for up to 20 ps in the microcanonical (NVE) ensemble. To better sample the initial conditions, a second NVE trajectory was started from the coordinates obtained 1 ps before the end of the NVT equilibration trajectory. Coordinates and velocities from each production run were saved every time step to ensure that the spectra at high frequencies do not get distorted.

The IR absorption coefficient was computed from the autocorrelation function (ACF) of the system's dipole moment time (t) derivative, $\langle \dot{\boldsymbol{\mu}}(0)\dot{\boldsymbol{\mu}}(t)\rangle$ (DACF), by taking its temporal Fourier transform. Thus, the spectrum obtained contains anharmonic effects that are generated as the trajectory moves on the (anharmonic) multidimensional potential energy surface.[24,25] Noise is reduced by averaging together the normalized spectra from each pair of trajectories that were started from different initial conditions. Missing from the picture, of course, are nuclear quantum effects because of the use of Newton's equations. The main effect involves the XH zero-point energy (here X = O or C) that is sometimes qualitatively accounted for by simply raising the temperature. In addition, a frequency-dependent nuclear "harmonic quantum correction" factor was applied to the computed IR intensities.[47] The vibrational frequencies were not corrected by any empirical factor.

In order to identify the absorption frequencies of the four water hydrogens and the shared one, H*, partial velocity autocorrelation functions (VACF) were calculated for each, by restricting the Fourier transform to the velocity of the specified H atom (the velocity is proportional to $\dot{\boldsymbol{\mu}}$ when interatomic charge transfer can be neglected).[25] See earlier work for a similar VACF application to protonated water clusters.[11,21,22]

RESULTS

The main results of this work are the static and dynamic IR spectra of the $H^+(H_2O)_2$(bz) cluster generated by Gaussian 09 and CP2K/AIMD, respectively. In both methods, we use predominantly DFT, with the above-mentioned functionals. In the static approach we also use the MP2(fc) method. These results are compared below with the experimental spectrum.

Optimized Geometries. As discussed above, the preparatory step for both methods involves generation of optimized molecular geometries in Gaussian 09 (Figure 1). Here we note that different functionals yield different isomers: (1) starting from the cZ isomer, the generalized gradient approximation (GGA) functionals (BLYP-D3 and PBE-D3) yield the cZ isomer (see Figure 1A). In contrast, the hybrid-GGA functionals (B3LYP-D3, PBE0-D3, and M06-2x) and the MP2(fc) method yield structures with an Eigen core. The fact that for these functionals cZ converged to a geometrically difference isomer (sE), rather than a cZ isomer with slightly different positions of the atoms, may indicate that cZ does not exist as a local minimum on the potential energy surface for these functionals. The sE structures obtained, Figure 1(panels C and E), are similar to those reported by the Duncan group,[23] with one H atom of the Eigen core attached to two adjacent bz carbon atoms, and its other two H atoms are H-bonded to an Ar atom and a water molecule. However, B3LYP-D3 yields an isomer that seems to be an intermediate between the sE and cZ isomers: one water molecule forms a bifurcated H-bond to two adjacent bz carbon atoms, while the other water molecule is close to the bridging position of the cZ isomer (see Figure 1, panels D and F). This new isomer is thus denoted E-Z. We note that an E-Z type isomer has previously been detected in the protonated water pentamer.[22] (2) Starting from the sE isomer, the PBE-D3 functional still converges to the cZ structure. In contrast, B3LYP-D3, PBE0-D3, M06-2x, and MP2(fc) yield the sE isomer, whereas BLYP-D3 yields the E-Z isomer.

The energies of the isomers are given in Table 1. Energies obtained in different methods are not really comparable. However, a sense of the energetic difference between isomers can be obtained by comparing the two BLYP and two B3LYP isomers (these are the only methods where we obtained more than a single global minimum). It can be seen that the E-Z isomer is higher in energy than either the sE and cZ isomers, although by only a small amount (<0.1 kcal/mol). It thus appears that sE and cZ are nearly isoenergetic, while E-Z is a kinetic intermediate connecting them.

Table 1. Energy (in Units of Hartree) of the sE, cZ, and E-Z Isomers of the $H^+(H_2O)_2$(bz)Ar Cluster Obtained from Gaussian 09 using DFT with Five Different Functionals and the MP2(fc) Method, All with the 6-311+G(d,p) Basis Set[a]

method	isomer	energy	ZPE	energy + ZPE	ΔE
PBE-D3	cZ	−912.44435	0.15628	−912.28807	
BLYP-D3	cZ	−912.99023	0.15566	−912.83457	0
BLYP-D3	E-Z	−912.99017	0.15573	−912.83443	0.085
B3LYP-D3	sE	−913.15352	0.16048	−912.99305	0
B3LYP-D3	E-Z	−913.15355	0.16062	−912.99293	0.073
PBE0-D3	sE	−912.51351	0.16178	−912.35174	
M06−2x	sE	−912.93056	0.16221	−912.76835	
MP2(fc)	sE	−911.45418	0.16181	−911.29236	

[a]ZPE represents the harmonic zero-point energy. ΔE is the energy difference (including ZPE) between isomers obtained at the same theory level (in kilocalories/mol).

DOI: 10.1021/jp509004j
J. Phys. Chem. B 2015, 119, 2658−2667

Table 2. Frequencies (in Inverse Centimeters) and Assignments for the Harmonic Normal Modes of the cZ Isomer of the $H_5O_2^+$(bz) Cluster (Excluding Benzene Modes), Obtained Using DFT/PBE-D3[32a]

mode	wavenumber	hydrogens	assignment
ν_1	3705	H_1, H_2	sym. OH stretch
ν_2	3703	H_1, H_2	asym. OH stretch
ν_3	3362	H_3, H_4	sym. OH stretch
ν_4	3312	H_3, H_4	asym. OH stretch
ν_5	1740	H*, H_3, H_4	H* perp. to bz ring, H_3, H_4 *gerade*
ν_6	1678	all	H* paral. to bz ring, *ungerade* water bend
ν_7	1550	all	H* perp. to bz ring, *gerade* water bend
ν_8	1345	H*, H_3, H_4	H* paral. to bz ring, H_3, H_4 *ungerade*
ν_9	1082	H*	excess proton mode

[a]These frequencies correlate with the nine highest energy modes of the gas-phase Zundel cation (i.e., they are not coupled to bz hydrogen modes). The dominant $H_5O_2^+$ hydrogen atoms contributing to each mode are listed, using the notations of Figure 1B. See Figure S11 of the Supporting Information.

The observation of essentially isoenergetic isomers suggests a flat potential energy surface with shallow minima. In such a case there could be many local minima, not all captured by an optimization procedure that starts from only three initial structures. The quantum chemistry packages do not provide a simple method for a more thorough conformational search, and it is not needed here because such a search is more naturally performed by MD simulations that, given sufficiently long simulation time, will sample all conformations below a prescribed energy.

The dynamical results are indeed more consistent. As the sE or cZ structures are equilibrated in CP2K (at 50 K), both end in the cZ geometry. In particular, when starting from a sE isomer (with the terminal water in either a *cis* or *trans* position), in three different density functionals, the geometry always changed to that of the cZ isomer. Interestingly, the E-Z isomer often appears as an intermediate between these two limiting structures (or as a fluctuation of the cZ isomer). This is demonstrated in movie files S1−S5 of the Supporting Information. Thus, dynamically there is only one isomer, cZ, and it is not the one assumed in the literature.[23]

Finally, it is amusing to note in these movies how the sE isomer, before reverting to the crouching position, executes several "walking" steps on the bz carbon skeleton. This occurs by first forming a "bifurcated" H-bond, in which a single water hydrogen donates a H-bond to two adjacent carbon atoms. When one of these cleaves, the sE isomer is often found standing on a different carbon atom.

Static Spectra. Figure 2 shows the computed harmonic IR spectra of the three isomers in comparison to the experimental spectrum shown in panel A. The normal-mode spectrum of the sE isomer is obtained using DFT with the PBE0-D3, B3LYP-D3, and M06-2x functionals, as well as MP2(fc), see panel D. There are shifts of up to 280 cm^{-1} between methods (attesting to the limited accuracy of the DFT functionals), but otherwise the spectra are similar to each other and to the results shown in Figure 3 of ref 23. These spectra seem to be quite remote from the experimental spectrum.

The harmonic spectra of the cZ isomer with and without Ar (panels B and C, respectively), was obtained with the BLYP-D3 and PBE-D3 functionals. The spectra from these 2 functionals are similar, with the BLYP-D3 spectrum slightly closer to the experimental spectrum. The spectra for the E-Z isomer, as obtained with the BLYP-D3 and B3LYP-D3 functionals, are shown in panel E. Again, they are similar to each other, with BLYP-D3 slightly closer to the experimentally detected bands. Taken together, these spectra point to the cZ or E-Z isomers as the dominant structures in the molecular beam, with the relative success of the BLYP functional attributed to a cancelation of errors.

Without the attached Ar atom (panel C), the cZ isomer maintains the C_2 symmetry of the isolated Zundel cation.[48] Its 9 normal modes originating from the 5 $H_5O_2^+$ hydrogen atoms ($3 \times 5 - 6 = 9$) are shown in Figure S11 of the Supporting Information, with assignments summarized in Table 2. These modes are adjusted to conform to the constraint of the bz plane. The highest four are contributed by the 4 water OH stretching modes. But instead of the primary coupling being between two H atoms of the same water molecule, as in the isolated Zundel cation, the dominant couplings here are intermolecular, between the free H atoms (H_1 and H_2) and between those H-bonded to the bz ring (H_3 and H_4).

The remaining 5 bands have frequencies below 2000 cm^{-1}, and they all involve the shared proton, H*. It can move either perpendicular to the bz ring (hence also perpendicular to the O−O axis), modes ν_5 and ν_7, or parallel to it (but still perpendicular to the O−O axis), modes ν_6 and ν_8. These four modes are coupled to the bending motion of the 4 water hydrogens as listed in Table 2. Then there is a single mode, ν_9, which is dominated by pure H* motion parallel to the O−O axis and is hence usually called the "proton transfer mode". Of these 5 bands, only two have high intensity: the proton transfer mode at 1082 cm^{-1} and the ν_6 mode at 1678 cm^{-1}, in which all 5 hydrogens move in concert.

With the symmetry breaking due to Ar attachment, each of the 4 outer hydrogens vibrates at a different frequency and they become nearly decoupled from each other. This is verified by the harmonic normal model analysis, shown in Figure S12 of the Supporting Information. The four highest-frequency normal modes, ν_1-ν_4, become almost local modes. The remaining 5 low frequency modes, that involve the excess proton, correlate with those shown in Table 2 with just small frequency shifts. An exception is the proton transfer mode, that shifts due to the Ar perturbation from 1082 to 1375 cm^{-1}. It likely corresponds to the experimental peak at 1488 cm^{-1}.

However, the system under consideration is highly anharmonic due to its floppy H-bonds. This effect must be accounted for. Therefore, we have also conducted anharmonic VPT2 calculations, shown in Figures S1−S8 and Tables S17−S32 of the Supporting Information. VPT2 often gives an improved description of spectra, such as recently demonstrated for the $H^+(H_2O)_{21}$ cluster.[39,49] Here, however, unreasonably

DOI: 10.1021/jp509004j
J. Phys. Chem. B 2015, 119, 2658−2667

large red-shifts are observed (also, blue shifts), occasionally accompanied by huge intensities. In addition, some of the low (harmonic) frequencies become imaginary in the VPT2 calculation [see footnote (28) in ref 39].

In particular, the H* band of the sE isomer at 2354 cm^{-1} (B3LYP) shifts all the way to 1490 cm^{-1}, and its amplitude becomes near infinite (see Figure S4 and Table S23 of the Supporting Information). While some red-shift was indeed anticipated,[23] the huge amplitude signals the possible breakdown of the perturbation expansion.

To check whether such a large shift is plausible, we consider the dependence of the OH frequency (ν_{OH}) on its average bond length (r_{OH}). The (nonlinear) dependence of the harmonic force constant on bond length is known as Badger's rule.[50,51] However, for OH bonds over a limited range, a nice linear dependence is observed[52] (see the straight line in Figure 3). Considering protonated water clusters, we find that the data (●) for H_3O^+ and the E-Z isomer of the $H^+(H_2O)_5$ cluster fall nearly on this line, whereas data for the Zundel cation constitute (nonlinear) extrapolation thereof. From the correlation, one expects that for r_{OH^*} = 1.046 Å (the MP2 distance in the sE cation), the frequency would be about 2500 cm^{-1}. It should not shift all the way to 1500 cm^{-1}, and hence, the VPT2 result is of suspicious validity for this band.

Since VPT2 is sensitive to the quality of the grid, we reoptimized and performed VPT2 anharmonic frequency analysis on Ar-tagged sE isomer at the B3LYP-D3/6-311+G-(d,p) level, by setting the grid to 199974 (the value of ultrafine grid is 99590) and the threshold for 2-electron integral accuracy to 10^{-12} (the default value is 10^{-10}). However, this refinement did not improve the anharmonic features. Large shifts, huge intensities, and imaginary frequencies still appear in the anharmonic IR spectrum (see Table S33 and Figure S9 of the Supporting Information). Conventional normal mode spectra therefore cannot reliably account for the anharmonicity here, and we switch to describe the dynamic results.

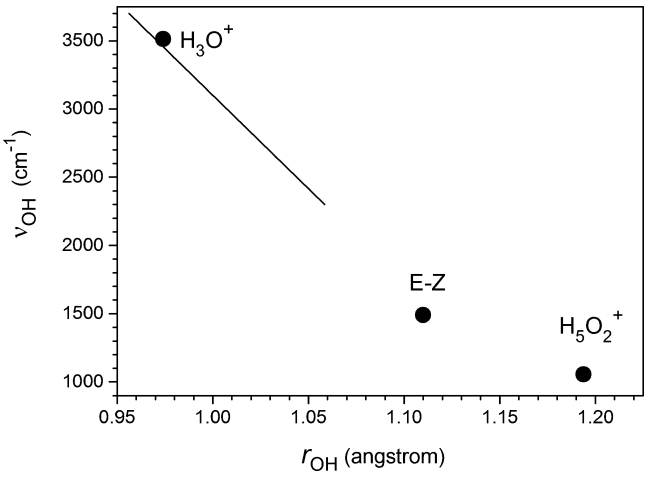

Figure 3. Dependence of OH stretch vibrational frequency, ν_{OH}, on its equilibrium (average) bond distance, r_{OH}. Line is the best fit result for neutral molecules:[52] r_{OH}(Å) = 1.226−7.29 × $10^{-5}\nu_{OH}(cm)^{-1}$. ● are data for gas-phase protonated water clusters, as follows: for H_3O^+, r_{OH} = 0.974 Å (experimental)[53] and ν_{OH} = 3514 cm^{-1} (asymmetric stretch).[54] For $H_5O_2^+$, r_{OH} = 1.1938 Å [CCSD(T)(FULL)][55] and ν_{OH} = 1047 cm^{-1} (Ne tagged).[15] For the E-Z pentameric cation,[22] $r_{OH} \approx$ 1.11 Å and ν_{OH} = 1490 cm^{-1} [Ar tagged $H^+(H_2O)_5$].[14]

Dynamic Spectra. In the dynamic approach,[24] one replaces the perturbation analysis of the potential near its global minimum with a trajectory that samples the portion of the potential that is accessible at the given total energy. The total dipole moment of the system is computed every time step. Its dot-product with its initial value (the DACF) is averaged and Fourier transformed to yield a dynamic IR spectrum which, by construction, includes anharmonic effects.

The AIMD spectra of the Ar-tagged cZ isomer with the PBE-D3, BLYP-D3, and B3LYP-D3 functionals are shown in Figure 4, panels B, C, and E, respectively. As already noted, the sE isomer converts to a cZ already in the equilibration step (for all three functionals), so there is only one isomer to be studied here. For all three functionals, the spectra are in semi-quantitative agreement with each other and with the experimental spectrum in panel A. In the high frequency region, above 3000 cm^{-1}, the IR spectrum from the B3LYP-D3 functional exhibits the best agreement with the experimental spectrum. There is the high-frequency triplet of peaks (blue-shifted by about 200 cm^{-1} as compared with the experimentally observed bands) and then the single peak around 3200 cm^{-1}

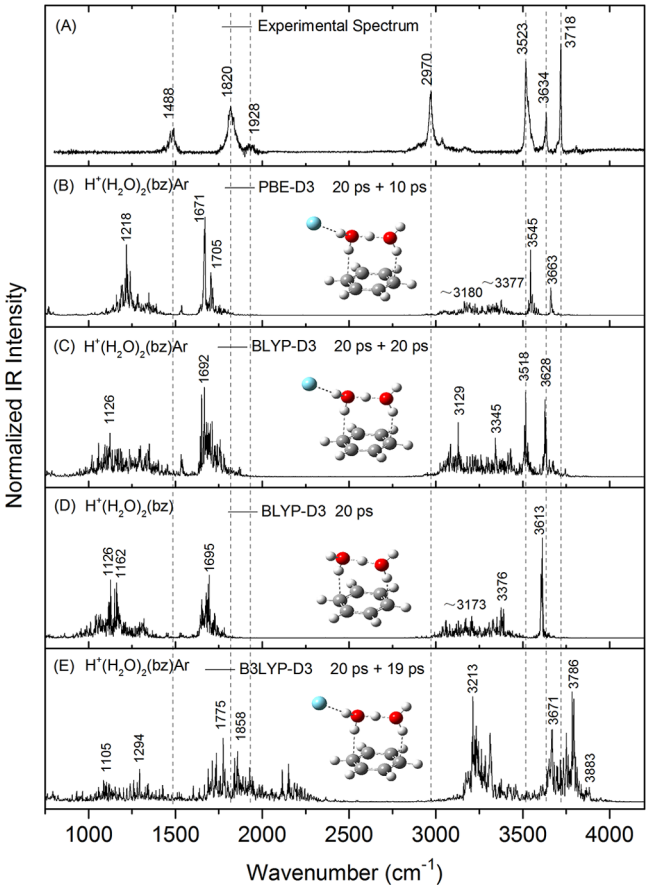

Figure 4. Dynamic IR spectra of the benzene-Zundel cluster: (A) The experimental photodissociation spectrum. Data from ref 23 (Figure 3). (B−E) Theoretical IR spectra of the "crouching Zundel" isomer obtained by averaging the (normalized) Fourier transforms of the DACF's from two AIMD/DFT production runs (of the indicated time lengths). (B) PBE-D3 functional for trajectory segments at T = 50 and 65 K. (C and D) BLYP-D3 at 50 K, with and without the Ar-tag, respectively (a single 20 ps trajectory was calculated here). (E) B3LYP-D3 at 50 K. Indicated peak frequencies are in inverse centimeters.

DOI: 10.1021/jp509004j
J. Phys. Chem. B 2015, 119, 2658−2667

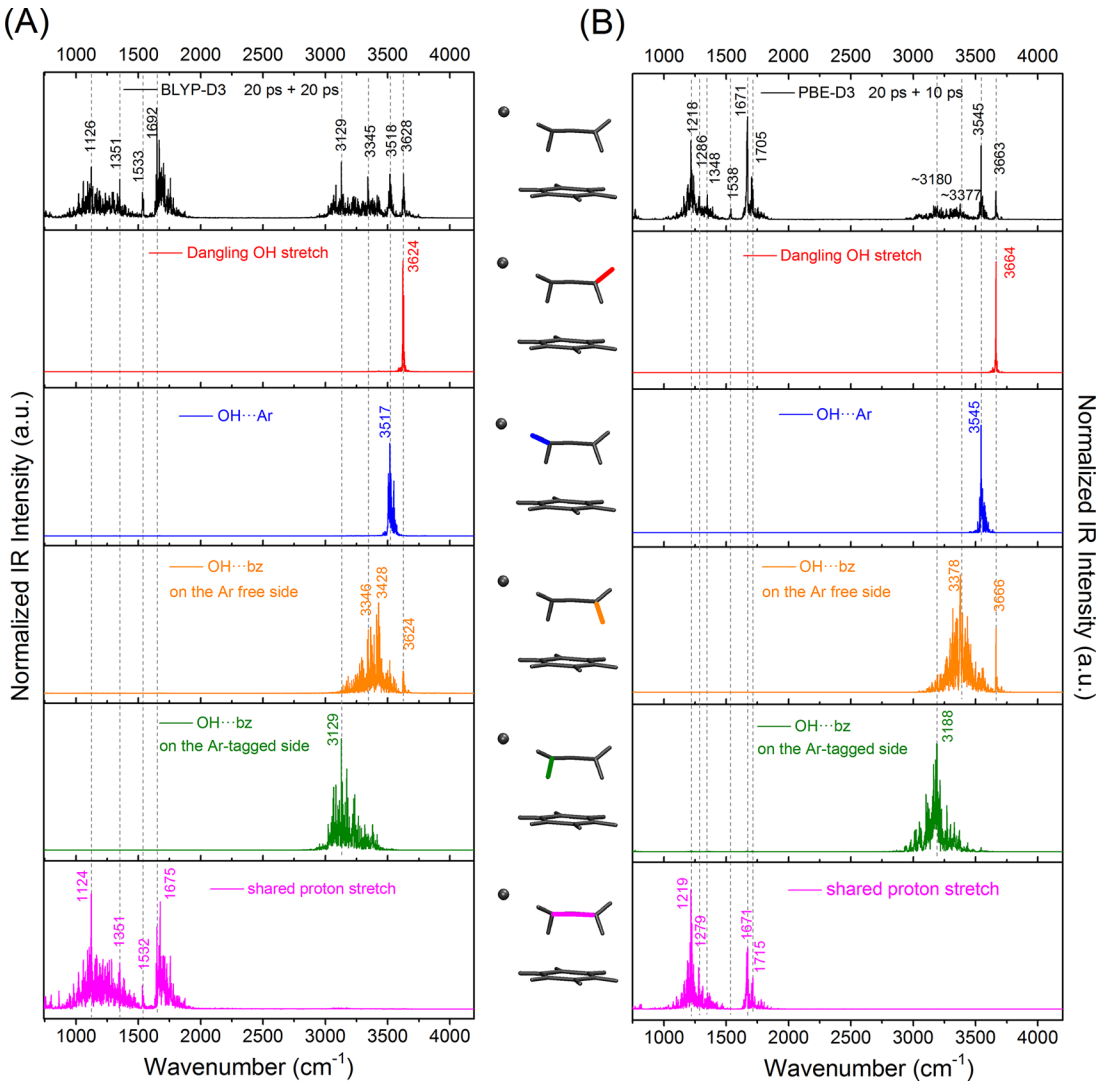

Figure 5. Simulated AIMD/DACF IR spectrum of the "crouching Zundel" isomer of the $H_5O_2^+$(bz)Ar cluster (top panel) is decomposed into the contributions from the 5 water hydrogen atoms using partial VACF analysis. Shown are DFT results with (A) the BLYP-D3 functional and (B) the PBE-D3 functional. The hydrogens are identified by the color code in the structures depicted between the two columns. A similar analysis of the cluster without Ar is shown in Figure S10 of the Supporting Information.

corresponding to the π-hydrogen bond observed experimentally at 2970 cm^{-1}. Most significant is the shared-proton region between 1000 and 2000 cm^{-1}. Here, all functionals show two clear peaks (around 1150 and 1700 cm^{-1}) that roughly correspond to the experimental ones at 1488 and 1820 cm^{-1}. Thus, these dynamic anharmonic spectra corroborate our earlier conclusion from the static harmonic spectra that the experimentally observed spectrum is preferably attributed to the cZ isomer.

As a reference, we also show in Figure 4D the AIMD spectrum of the untagged cluster. What is especially evident here is that the peaks below 2000 cm^{-1} are similar to those of the bare Zundel cation,[14,15,20,48] so that the bz ring is a small perturbation for the shared-proton dynamics.

VACF Peak Assignments. To aid in assigning the vibrational bands of the dynamic spectra, we have calculated from our AIMD trajectories also the (partial) velocity autocorrelation functions (VACF's) for each of the five $H_5O_2^+$ hydrogens, Fourier transforming them to elucidate the IR bands to which each proton contributes. Figure 5 shows the results for the Ar-tagged cluster for the two DFT functionals (BLYP-D3 and PBE-D3) in its two columns (left and right, respectively). The top row shows the full DACF spectrum (Figure 4) for the Ar-tagged cZ cation. The five rows below it show the (Fourier transformed) partial VCAF's of the 5 hydrogens, color coded as indicated on the stick structures of this cluster. Focusing on the BLYP results (left column), we see that they can be ordered by their red-shifted OH band as follows: Dangling (non-H-bonded) OH_1 at 3628 cm^{-1}; OH_2···Ar at 3518 cm^{-1}; OH_3···bz on the Ar-free side at 3345 cm^{-1}; OH_4···bz on the Ar-tagged side at ca. 3129 cm^{-1}; and shared proton, O···H*···O, near both the 1700 and 1200 cm^{-1} DACF bands.

The fact that the shared proton does not absorb at only a single frequency has been noted before.[11,21,22] The above ordering follows the order of increasing OH bond lengths in Figure 1B, although the differences there are not always significant enough to explain the shifts quantitatively. This assignment is also in agreement with the normal-mode analysis from Table 2 and Figure S11 of the Supporting Information.

DOI: 10.1021/jp509004j
J. Phys. Chem. B 2015, 119, 2658−2667

DISCUSSION AND CONCLUSIONS

A protonated water dimer on a benzene molecule can assume two main geometries, perpendicular and parallel to the aromatic ring. In the perpendicular geometry, only one of the water molecules contacts the benzene ring. It has a structure similar to H_3O^+ (that is solvated by three ligands) and hence described by us as a "standing Eigen" cation. This is the only isomer previously considered to exist in the molecular beam.[23]

In the parallel geometry both water molecules contact the benzene ring. Hence the protonated dimer is solvated symmetrically and the excess proton is equally shared in this "crouching Zundel" isomer. Although not previously considered, it appears to agree best with the experimental IR spectrum of the $H_5O_2^+$(bz)Ar ion. This is based on computations of both static and dynamic spectra for these isomers.

DFT calculations with Gaussian 09 optimize to the sE isomer with some DFT functionals and to the cZ isomer with others. Occasionally, two local minima are found. The second one is then a third isomer with structure intermediate between the Eigen and Zundel isomers (and hence termed E-Z). MP2 also favors the sE isomer. However, in the dynamic simulations, we always obtain the cZ isomer, whose fluctuations likely encompass also the E-Z structure. Possibly it gains extra stability (lower free energy) by proton delocalization within its Zundel core.

The static harmonic spectra of the cZ isomer are in better agreement with the experimental spectrum than those of the sE isomer. VPT2 anharmonicities in this case are suspect because for some of the dominant modes they result in excessive shifts, imaginary frequencies or huge intensities. However, in the MP2 anharmonic spectrum for the sE isomer, only few low frequency modes are problematic (Tables S31 and S32 of the Supporting Information) and agreement with the experiment is rather good (Figure S8 of the Supporting Information). Judging from this VPT2 result, the sE isomer might also be present in the molecular beam.

However, a more reliable method for treating anharmonicities in this case is the dynamic one, based on AIMD trajectories in CP2K. Here trajectories with either the BLYP, PBE, or B3LYP functional thermalize to yield the cZ isomer, whose DACF spectrum is in semiquantitative agreement with experiment. The agreement is clearly limited by the accuracy of the density functionals.

Thus, this system is challenging in spite of its "small" size, because (a) the optimized structures are different for different functionals, (b) the anharmonic VPT2 results are probably not reliable here, and (c) the AIMD/DACF spectra do not reproduce the experimental spectrum quantitatively, perhaps due to limited DFT accuracy.

Hopefully when it becomes feasible to run AIMD with truly ab initio methods such as MP2, a more quantitative comparison will emerge. Quantum (nuclear) effects are also anticipated to play an important role in these clusters.

Finally, we have also calculated the partial VACF spectra for each of the five hydrogens of the $H_5O_2^+$ entity and mapped out the order of their red-shifts (Figure 5). The highest frequency is due to the dangling H then come the Ar-bound and bz-bound hydrogens. The most red-shifted, of course, is the shared proton that contributes strongly below 2000 cm^{-1}. This agrees with the normal-mode assignments in Table 2.

The main conclusion, namely that the dominant isomer is the one with a Zundel (rather than Eigen) core, is in line with recent results for the protonated water tetramer[21] and pentamer.[22] Their experimental IR spectra are best explained if instead of (or in addition to) the branched Eigen isomer one assumes a contribution from a linear Zundel isomer. It thus appears that a Zundel core is more prevalent in small clusters than previously anticipated. Possibly, the lack of water molecules to delocalize the charge in the Eigen cation (e.g., by the special pair dance)[13] accentuates the importance of the charge delocalization between the oxygen atoms of the protonated water dimer, and hence its enhanced significance in low dimensional systems.

It is perhaps dangerous to project from such a small system to the case of protons in proteins or at interfaces. Therefore, the following are only tentative ideas. A possibility to consider is that interfacial protons assume the cZ geometry. They would therefore lie along the interfacial plane, forming linear water chains through H-bonds to the dangling hydrogens seen in Figure 1B. This could lead to fast proton migration in the interfacial water layer.[2,3] Additionally, proton escape to the bulk would be impeded by the need to reorganize a large number of water molecules around the interfacial Zundel cation to allow for its proper resolvation as a bulklike Eigen cation.

ASSOCIATED CONTENT

Supporting Information

PDF with Tables S1−S16, optimized cluster coordinates; Tables S17−S32, harmonic and anharmonic (VPT2) fundamentals; Table S33, anharmonic (VPT2) fundamentals with refined grid; Tables S34 and S35, harmonic normal mode assignments; Figures S1−S8, VPT2 anharmonic spectra; Figure S9, VPT2 anharmonic spectrum of sE isomer with refined grid; Figure S10, VACF analysis of the untagged isomer; Figures S11 and S12, harmonic normal modes of the cZ isomer. Movie files S1−S5, ca. 5 ps NVT equilibration trajectories of an initially "standing Eigen" isomer at 50 K with different functionals and starting geometries: S1 and S2, BLYP-D3 functional with terminal water initially *cis* or *trans* to the benzene ring, respectively; Movies S3 and S4, PBE-D3 functional (S3 *cis* and S4 *trans*); Movie S5, B3LYP-D3 functional (*cis* sE). This material is available free of charge via the Internet at http://pubs.acs.org.

AUTHOR INFORMATION

Corresponding Author

*E-mail: agmon@fh.huji.ac.il.

Notes

The authors declare no competing financial interest.

ACKNOWLEDGMENTS

We are indebted to Michael A. Duncan for the experimental data in Figures 2A and 4A. This research was supported by a Golda Meir Fellowship to H.W. and US-Israel Binational Science Foundation (BSF) Grant 2010250. The Fritz Haber Center is supported by the Minerva Gesellschaft für die Forschung, München, FRG.

REFERENCES

(1) Wraight, C. A. Chance and Design−Proton Transfer in Water, Channels and Bioenergetic Proteins. *Biochim. Biophys. Acta* **2006**, *1757*, 886−912.

(2) Springer, A.; Hagen, V.; Cherepanov, D. A.; Antonenko, Y. N.; Pohl, P. Protons Migrate along Interfacial Water without Significant Contributions from Jumps between Ionizable Groups on the

DOI: 10.1021/jp509004j
J. Phys. Chem. B 2015, 119, 2658−2667

Membrane Surface. *Proc. Natl. Acad. Sci. U.S.A.* **2011**, *108*, 14461−14466.
(3) Zhang, C.; Knyazev, D. G.; Vereshaga, Y. A.; Ippoliti, E.; Nguyen, T. H.; Carloni, P.; Pohl, P. Water at Hydrophobic Interfaces Delays Proton Surface-to-Bulk Transfer and Provides a Pathway for Lateral Proton Diffusion. *Proc. Natl. Acad. Sci. U.S.A.* **2012**, *109*, 9744−9749.
(4) Agmon, N.; Gutman, M. Bioenergetics: Proton Fronts on Membranes. *Nat. Chem.* **2011**, *3*, 840−842.
(5) Petersen, P. B.; Saykally, R. J. Evidence for an Enhanced Hydronium Concentration at the Liquid Water Surface. *J. Phys. Chem. B* **2005**, *109*, 7976−7980.
(6) Petersen, M. K.; Iyengar, S. S.; Day, T. J. F.; Voth, G. A. The Hydrated Proton at the Water Liquid/Vapor Interface. *J. Phys. Chem. B* **2004**, *108*, 14804−14806.
(7) Buch, V.; Milet, A.; Vácha, R.; Jungwirth, P.; Devlin, J. P. Water Surface is Acidic. *Proc. Nat. Acad. Sci., U.S.A.* **2007**, *104*, 7342−7347.
(8) Petersen, M. K.; Voth, G. A. Amphiphilic Character of the Hydrated Proton in Methanol-Water Solutions. *J. Phys. Chem. B* **2006**, *110*, 7085−7089.
(9) Kumar, R.; Knight, C.; Voth, G. A. Exploring the Behaviour of the Hydrated Excess Proton at Hydrophobic Interfaces. *Faraday Discuss.* **2013**, *167*, 263−278.
(10) Yamashita, T.; Voth, G. A. Properties of Hydrated Excess Protons near Phospholipid Bilayers. *J. Phys. Chem. B* **2010**, *114*, 592−603.
(11) Kulig, W.; Agmon, N. A 'Clusters-in-Liquid' Method for Calculating Infrared Spectra Identifies the Proton Transfer Mode in Acidic Aqueous Solution. *Nat. Chem.* **2013**, *5*, 29−35.
(12) Yeh, L. I.; Okumura, M.; Myers, J. D.; Price, J. M.; Lee, Y. T. Vibrational Spectroscopy of the Hydrated Hydronium Cluster Ions $H_3O^+\cdot(H_2O)_n$ (n = 1,2,3). *J. Chem. Phys.* **1989**, *91*, 7319−7330.
(13) Markovitch, O.; Chen, H.; Izvekov, S.; Paesani, F.; Voth, G. A.; Agmon, N. Special Pair Dance and Partner Selection: Elementary Steps in Proton Transport in Liquid Water. *J. Phys. Chem. B* **2008**, *112*, 9456−9466.
(14) Headrick, J. M.; Diken, E. G.; Walters, R. S.; Hammer, N. I.; Christie, R. A.; Cui, J.; Myshakin, E. M.; Duncan, M. A.; Johnson, M. A.; Jordan, K. D. Spectral Signatures of Hydrated Proton Vibrations in Water Clusters. *Science* **2005**, *308*, 1765−1769.
(15) Hammer, N. I.; Diken, E. G.; Roscioli, J. R.; Johnson, M. A.; Myshakin, E. M.; Jordan, K. D.; McCoy, A. B.; Huang, X.; Bowman, J. M.; Carter, S. The Vibrational Predissociation Spectra of the $H_5O_2^+\cdot Rg_n$ (Rg = Ar, Ne) Clusters: Correlation of the Solvent Perturbations in the Free OH and Shared Proton Transitions of the Zundel Ion. *J. Chem. Phys.* **2005**, *122*, 244301.
(16) Douberly, G. E.; Walters, R. S.; Cui, J.; Jordan, K. D.; Duncan, M. A. Infrared Spectroscopy of Small Protonated Water Clusters, $H^+(H_2O)_n$ (n = 2−5): Isomers, Argon Tagging, and Deuteration. *J. Phys. Chem. A* **2010**, *114*, 4570−4579.
(17) Olesen, S. G.; Guasco, T. L.; Roscioli, J. R.; Johnson, M. A. Tuning the Intermolecular Proton Bond in the $H_5O_2^+$ 'Zundel Ion' Scaffold. *Chem. Phys. Lett.* **2011**, *509*, 89−95.
(18) Mizuse, K.; Fujii, A. Tuning of the Internal Energy and Isomer Distribution in Small Protonated Water Clusters $H^+(H_2O)_{4-8}$: An Application of the Inert Gas Messenger Technique. *J. Phys. Chem. A* **2012**, *112*, 4868−4877.
(19) McCoy, A. B.; Guasco, T. L.; Leavitt, C. M.; Olesen, S. G.; Johnson, M. A. Vibrational Manifestations of Strong Non-Condon Effects in the $H_3O^+\cdot X_3$ (X = Ar, N_2, CH_4, H_2O) Complexes: A Possible Explanation for the Intensity in the "Association Band" in the Vibrational Spectrum of Water. *Phys. Chem. Chem. Phys.* **2012**, *14*, 7205−7214.
(20) Asmis, K. R.; Pivonka, N. L.; Santambrogio, G.; Brümmer, M.; Kaposta, C.; Neumark, D. M.; Wöste, L. Gas-Phase Infrared Spectrum of the Protonated Water Dimer. *Science* **2003**, *299*, 1375−1377.
(21) Kulig, W.; Agmon, N. Both Zundel and Eigen Isomers Contribute to the IR Spectrum of the Gas-Phase $H_9O_4^+$ Cluster. *J. Phys. Chem. B* **2014**, *118*, 278−286.
(22) Kulig, W.; Agmon, N. Deciphering the Infrared Spectrum of the Protonated Water Pentamer and the Hybrid Eigen-Zundel Cation. *Phys. Chem. Chem. Phys.* **2014**, *16*, 4933−4941.
(23) Cheng, T. C.; Bandyopadhyay, B.; Mosley, J. D.; Duncan, M. A. IR Spectroscopy of Protonation in Benzene-Water Nanoclusters: Hydronium, Zundel, and Eigen at a Hydrophobic Interface. *J. Am. Chem. Soc.* **2012**, *134*, 13046−13055.
(24) Berens, P. H.; Wilson, K. R. Molecular Dynamics and Spectra. I. Diatomic Rotation and Vibration. *J. Chem. Phys.* **1981**, *74*, 4872−4882.
(25) Gaigeot, M.-P.; Martinez, M.; Vuilleumier, R. Infrared Spectroscopy in the Gas and Liquid Phase from First Principle Molecular Dynamics Simulations: Application to Small Peptides. *Mol. Phys.* **2007**, *105*, 2857−2878.
(26) Cimas, A.; Vaden, T. D.; de Boer, T. S. J. A.; Snoek, L. C.; Gaigeot, M.-P. Vibrational Spectra of Small Protonated Peptides from Finite Temperature MD Simulations and IRMPD Spectroscopy. *J. Chem. Theory Comput.* **2009**, *5*, 1068−1078.
(27) Gaigeot, M.-P. Theoretical Spectroscopy of Floppy Peptides at Room Temperature. A DFTMD Perspective: Gas and Aqueous Phase. *Phys. Chem. Chem. Phys.* **2010**, *12*, 3336−3359.
(28) Rossi, M.; Blum, V.; Kupser, P.; von Helden, G.; Bierau, F.; Pagel, K.; Meijer, G.; Scheffler, M. Secondary Structure of Ac-Ala-LysH^+ Polyalanine Peptides (n = 5, 10, 15) in Vacuo: Helical or Not? *J. Phys. Chem. Lett.* **2010**, *1*, 3465−3470.
(29) Park, M.; Shin, I.; Singh, N. J.; Kim, K. S. Eigen and Zundel Forms of Small Protonated Water Clusters: Structures and Infrared Spectra. *J. Phys. Chem. A* **2007**, *111*, 10692−10702.
(30) Yu, H.; Cui, Q. The Vibrational Spectra of Protonated Water Clusters: A Benchmark for Self-Consistent-Charge Density-Functional Tight Binding. *J. Chem. Phys.* **2007**, *127*, 234504.
(31) Heine, N.; Fagiani, M. R.; Rossi, M.; Wende, T.; Berden, G.; Blum, V.; Asmis, K. R. Isomer-Selective Detection of Hydrogen-Bond Vibrations in the Protonated Water Hexamer. *J. Am. Chem. Soc.* **2013**, *135*, 8266−8273.
(32) Frisch, M. J.; Trucks, G. W.; Schlegel, H. B.; Scuseria, G. E.; Robb, M. A.; Cheeseman, J. R.; Scalmani, G.; Barone, V.; Mennucci, B.; Petersson, G. A. et al. Gaussian 09 Revision D.01. Gaussian Inc.: Wallingford, CT, 2013.
(33) Perdew, J. P.; Burke, K.; Ernzerhof, M. Generalized Gradient Approximation Made Simple. *Phys. Rev. Lett.* **1996**, *77*, 3865−3868.
(34) Adamo, C.; Barone, V. Toward Reliable Density Functional Methods without Adjustable Parameters: The PBE0 Model. *J. Chem. Phys.* **1999**, *110*, 6158−6170.
(35) Miehlich, B.; Savin, A.; Stoll, H.; Preuss, H. Results Obtained with the Correlation Energy Density Functionals of Becke and Lee, Yang and Parr. *Chem. Phys. Lett.* **1989**, *157*, 200−206.
(36) Becke, A. D. Density-Functional Exchange-Energy Approximation with Correct Asymptotic Behavior. *Phys. Rev. A* **1988**, *38*, 3098−3100.
(37) Lee, C.; Yang, W.; Parr, R. G. Development of the Cole-Salvetti Correlation Energy Formula into a Function of the Electron Density. *Phys. Rev. B* **1988**, *37*, 785−789.
(38) Zhao, Y.; Truhlar, D. G. The M06 Suite of Density Functionals for Main Group Thermochemistry, Thermochemical Kinetics, Noncovalent Interactions, Excited States, and Transition Elements: Two New Functionals and Systematic Testing of Four M06-Class Functionals and 12 Other Functionals. *Theor. Chem. Acc.* **2008**, *120*, 215−241.
(39) Torrent-Sucarrat, M.; Anglada, J. M. Anharmonicity and the Eigen-Zundel Dilemma in the IR Spectrum of the Protonated 21 Water Cluster. *J. Chem. Theory Comput.* **2011**, *7*, 467−472.
(40) Bloino, J.; Barone, V. A Second-Order Perturbation Theory Route to Vibrational Averages and Transition Properties of Molecules: General Formulation and Application to Infrared and Vibrational Circular Dichroism Spectroscopies. *J. Chem. Phys.* **2012**, *136*, 124108.
(41) VandeVondele, J.; Krack, M.; Mohamed, F.; Parrinello, M.; Chassaing, T.; Hutter, J. QUICKSTEP: Fast and Accurate Density Functional Calculations Using a Mixed Gaussian and Plane Waves Approach. *Comput. Phys. Commun.* **2005**, *167*, 103−128.

DOI: 10.1021/jp509004j
J. Phys. Chem. B 2015, 119, 2658−2667

(42) Grimme, S.; Antony, J.; Ehrlich, S.; Krieg, H. A Consistent and Accurate Ab Initio Parametrization of Density Functional Dispersion Correction (DFT-D) for the 94 Elements H-Pu. *J. Chem. Phys.* **2010**, *132*, 154104.
(43) Goedecker, S.; Teter, M.; Hutter, J. Separable Dual-Space Gaussian Pseudopotentials. *Phys. Rev. B* **1996**, *54*, 1703−1710.
(44) Martyna, G. J.; Tuckerman, M. E. A Reciprocal Space Based Method for Treating Long Range Interactions in Ab Initio and Force-Field-Based Calculations in Clusters. *J. Chem. Phys.* **1999**, *110*, 2810−2821.
(45) VandeVondele, J.; Hutter, J. An Efficient Orbital Transformation Method for Electronic Structure Calculations. *J. Chem. Phys.* **2003**, *118*, 4365−4369.
(46) Nosé, S. A Molecular Dynamics Method for Simulations in the Canonical Ensemble. *Mol. Phys.* **1984**, *52*, 255−268.
(47) Ramírez, R.; López-Ciudad, T.; Kumar, P.; Marx, D. Quantum Corrections to Classical Time-Correlation Functions: Hydrogen Bonding and Anharmonic Floppy Modes. *J. Chem. Phys.* **2004**, *121*, 3972−3983.
(48) Vendrell, O.; Gatti, F.; Meyer, H.-D. Full Dimensional (15-Dimensional) Quantum-Dynamical Simulation of the Protonated Water Dimer. II. Infrared Spectrum and Vibrational Dynamics. *J. Chem. Phys.* **2007**, *127*, 184303.
(49) Fournier, J. A.; Johnson, C. J.; Wolke, C. T.; Weddle, G. H.; Wolk, A. B.; Johnson, M. A. Vibrational Spectral Signature of the Proton Defect in the Three-Dimensional $H^+(H_2O)_{21}$ Cluster. *Science* **2014**, *344*, 1009−1012.
(50) Badger, R. M. A Relation Between Internuclear Distances and Bond Force Constants. *J. Chem. Phys.* **1934**, *2*, 128−131.
(51) Cioslowski, J.; Liu, G.; Castro, R. A. M. Badger's Rule Revisited. *Chem. Phys. Lett.* **2000**, *331*, 497−501.
(52) Demaison, J.; Herman, M. Lievin, The Equilibrium OH Bond Length. *Int. Rev. Phys. Chem.* **2007**, *26*, 391−420.
(53) Tang, J.; Oka, T. Infrared Spectroscopy of H_3O^+: The ν_1 Fundamental Band. *J. Mol. Spectrosc.* **1999**, *196*, 120−130.
(54) Begemann, M. H.; Gudeman, C. S.; Pfaff, J.; Saykally, R. J. Detection of the Hydronium Ion (H_3O^+) by High-Resolution Infrared Spectroscopy. *Phys. Rev. Lett.* **1983**, *51*, 554−557.
(55) Auer, A. A.; Helgaker, T.; Klopper, W. Accurate Molecular Geometries of the Protonated Water Dimer. *Phys. Chem. Chem. Phys.* **2000**, *2*, 2235−2238.

DOI: 10.1021/jp509004j
J. Phys. Chem. B 2015, 119, 2658−2667